

Connecting baryon light-front wave functions to quasi-transverse-momentum-dependent correlators in lattice QCD

Simone Rodini,^{1,2,*} Andrea Schiavi,^{1,2,†} and Barbara Pasquini^{1,2,‡}

¹*Dipartimento di Fisica "A. Volta", Università degli Studi di Pavia, I-27100 Pavia, Italy*

²*Istituto Nazionale di Fisica Nucleare, Sezione di Pavia, I-27100 Pavia, Italy*

(Dated: March 10, 2026)

Within light-front quantization, hadrons can be represented on a Fock-space basis of configurations of elementary partons. The coefficients of the expansion are called light-front wave functions (LFWFs), and encode all the dynamical degrees of freedom. We show how to extract the LFWFs of baryons, such as the proton, from equal-time correlators suitable for Lattice QCD simulations. Using an operator product expansion, we prove the factorization of the relevant correlator in the three-quark color-singlet LFWF, a residual lattice factor, and a soft factor that systematically subtracts the additional divergences arising from the factorization. We verify up to next-to-leading order the independent renormalizability of the LFWF, and we derive the evolution equations that govern its scale dependence.

I. INTRODUCTION

Quantum Chromodynamics (QCD) provides the fundamental description of the strong interaction between quarks and gluons, collectively referred to as partons. Due to confinement, these degrees of freedom cannot be observed as free particles, but only as constituents of color-singlet bound states called hadrons. While asymptotic freedom allows for a perturbative treatment of QCD at high energies, it remains an open problem the nonperturbative dynamics, which is responsible for the formation and internal structure of the hadrons.

A natural framework to discuss hadron structure is light-front quantization, where hadron states are expanded on a Fock-space basis of parton configurations, with coefficients given by light-front wave functions (LFWFs). These encode the full momentum-space structure of the parton configurations, and, in principle, contain all the information on the internal dynamics of the bound states. In particular, experimentally measurable quantities such as parton distribution functions can be described as products of LFWFs where some parton degrees of freedom are integrated out. These distributions therefore focus on specific aspects of the more complete information contained in the LFWFs, which, in this sense, represent the most fundamental nonperturbative quantities describing hadron structure.

In this paper, we work directly on the LFWFs as the central nonperturbative objects. However, the form of the QCD light-front Hamiltonian for the bound-state eigenvalue problem is not known, preventing a direct determination of the LFWFs. Thus, we turn to Lattice QCD, which allows for first-principle nonperturbative calculations of hadronic matrix elements by formulating QCD in Euclidean spacetime on a bounded and discrete grid. Lattice simulations give access to equal-time correlators, therefore dedicated factorization theorems are required to connect them to the light-front amplitudes we are interested in. The factorization produces additional divergences that must cancel in physical observables, and requires the nonperturbative quantities to be renormalizable independently of lattice artefacts. Factorization frameworks have been developed for transverse-momentum-dependent (TMD) parton distribution and fragmentation functions [1, 2] as well as generalized parton distributions (see, e.g., reviews [3–6] and references therein), and meson LFWFs [7–9]. In this work, we extend this program to the LFWFs of baryons, most notably the proton, isolating the relevant partonic degrees of freedom through a TMD operator expansion based on the background field method [10, 11].

The paper is organized as follows. In Sec. II, we define the proper equal-time correlator on the lattice, called a quasi-transverse-momentum-dependent (QTMD) correlator, and present the TMD expansion at leading power. In Sec. III, we analyze the structure of divergences of the factorized QTMD correlator, which is composed of the three-quark baryon LFWF, a residual lattice factor, and a soft factor to compensate the additional divergences arising from the factorization [12, 13]. Alongside ultraviolet divergences, there are rapidity divergences coming from the interaction of the original fields with lightlike gauge links at infinity. In Sec. IV, we prove the cancellation of these divergences at next-to-leading order, and the independent renormalizability of the physical LFWF. This is a function of one ultraviolet renormalization scale, alongside one rapidity scale for each quark, with independent evolution with respect

* Electronic address: simone.rodini@unipv.it

† Electronic address: andrea.schiavi01@universitadipavia.it

‡ Electronic address: barbara.pasquini@unipv.it

to each of them, which we prove in Sec. V. In Sec. VI, we summarize our results, and conclude by commenting on possible future developments.

II. THE QTMD CORRELATOR

To connect the leading three-quark LFWF of a baryon to a quantity that can be studied within the framework of Lattice QCD, consider a spacetime event of the form

$$y = lv + b, \quad (1)$$

where, using decomposition (A1), $b = b_\perp = y_\perp$, and, without loss of generality, we can choose v as

$$v = \frac{n - \bar{n}}{\sqrt{2}} = \frac{1}{\sqrt{2}}(-1, 1, 0, 0). \quad (2)$$

Given a baryon with four-momentum P and spin S , we define the QTMD correlator as

$$\tilde{\Omega}_v(y_1, y_2, y_3; P, S) = \langle 0 | \varepsilon_{ijk} J_{v,i}(y_1) J_{v,j}(y_2) J_{v,k}(y_3) | P, S \rangle, \quad (3)$$

where antisymmetrization over fundamental-representation color indices i, j, k is implied. The current J is defined as

$$J_v(y) = [Lv + L_\perp, Lv + y_\perp] [Lv + y_\perp, y] q(y), \quad (4)$$

where q is a quark field operator, and $[y_2, y_1]$ is the Wilson line between two spacetime events y_1, y_2 , defined as

$$[y_2, y_1] = P \left[\exp \left(ig \int_{y_1}^{y_2} dy^\mu A_\mu(y) \right) \right], \quad (5)$$

with g the strong coupling constant, A_μ the gluon field operator, and $P[\dots]$ the path-ordering operator. In Eq. (4), L, L_\perp are finite on the lattice, but are assumed to be much bigger than every l, b , allowing us to treat them effectively as infinite in calculations. For this reason, the current is referred to as a semicompact operator. We consider $\text{sign}(L) = -1, +1$ for an hadron in the initial or final state, respectively, with the two versions of the baryon QTMD correlator represented in Fig. 1. Since the QTMD correlator is defined at equal time, it can be directly formulated on a Euclidean lattice; moreover, it can be expressed as a path integral, i.e.,

$$\tilde{\Omega}_v(y_1, y_2, y_3; P, S) = \int [DqDA] e^{iS_{\text{QCD}}[q,A]} \varepsilon_{ijk} J_{v,i}(y_1) J_{v,j}(y_2) J_{v,k}(y_3) \phi(P, S), \quad (6)$$

where S_{QCD} is the QCD action, and ϕ is the baryon field.

Consider

$$P = P^+ \bar{n} + \frac{M^2}{2P^+} n, \quad (7)$$

where $M \ll P^+$ is the mass of the baryon. Using the background field method [10] with two background fields adapted to a TMD expansion [11], we shift the fields as

$$q \mapsto \psi + q_{\bar{n}} + q_v, \quad A^\mu \mapsto B^\mu + A_{\bar{n}}^\mu + A_v^\mu, \quad (8)$$

where ψ, B^μ are dynamical fields, while the remaining ones are treated as background. The \bar{n} -collinear fields, which are almost collinear to the baryon, are required to satisfy the scaling relations

$$(\partial^+, \partial^-, \partial_\perp)(q_{\bar{n}}, A_{\bar{n}}) \lesssim (1, \lambda^2, \lambda) P^+(q_{\bar{n}}, A_{\bar{n}}), \quad (9)$$

with

$$\lambda = (M/P^+) \ll 1. \quad (10)$$

Central to our study is the ability to retain the dependence on the transverse momentum of the partons. To this end, we allow the transverse field separations inside the baryon to be large, namely of the order of $b \sim (1/M) = (\lambda P^+)^{-1}$.

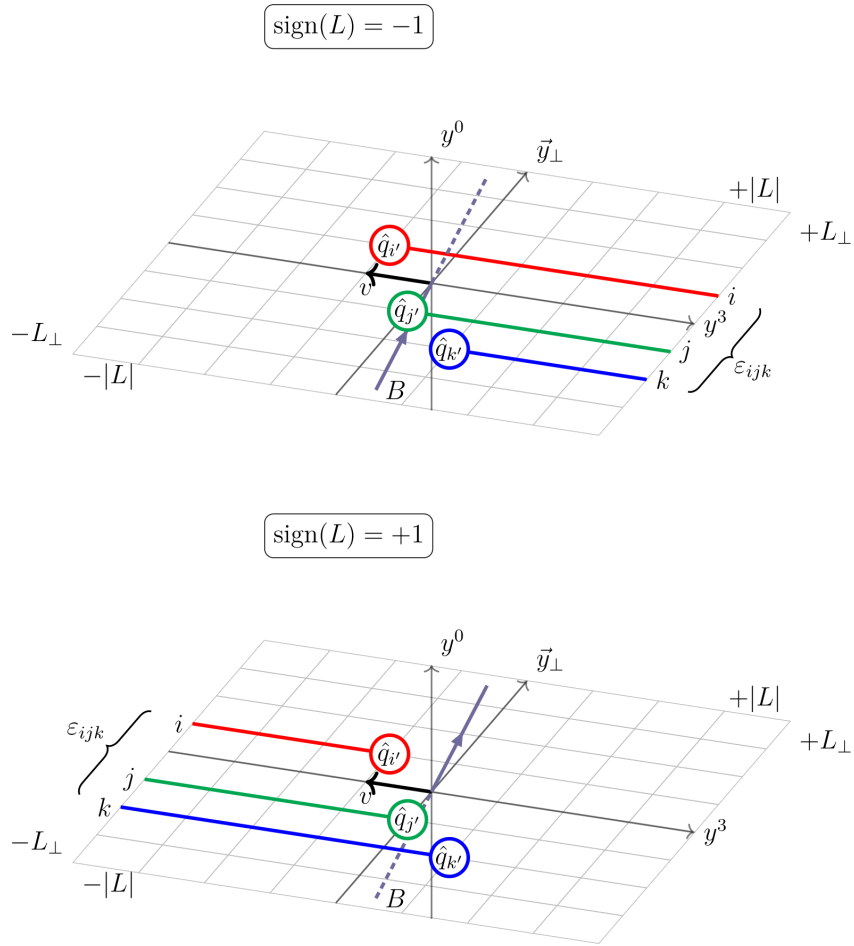


Figure 1. Baryon QTMD correlator. We consider the baryon B traveling along the y^3 -axis, and the quark operators \hat{q} on the hypersurface $y^0 = 0$ are connected to the boundary of the lattice through Wilson lines. The lattice is bounded by $|L|$ along the y^3 -axis, and by L_\perp along the perpendicular spatial directions. The cases $\text{sign}(L) = -1, +1$ correspond to a baryon in the initial and final state, respectively. For simplicity, we only represent the v -directed gauge links, colored in red, green and blue to visually indicate the antisymmetrization of the color indices in the fundamental representation.

Therefore, terms of the form $b^\mu \partial_\mu (q_{\bar{n}}, A_{\bar{n}}) \sim (q_{\bar{n}}, A_{\bar{n}})$ cannot be ignored. We still require a suppression of the anti-collinear momentum, i.e., $y^+ \partial^- (q_{\bar{n}}, A_{\bar{n}}) \sim \lambda (q_{\bar{n}}, A_{\bar{n}})$ or smaller. At the same time, to stay away from the small- x regime, where x is the fraction of longitudinal momentum of the baryon carried by a parton, we want to keep $y^- \partial^+ (q_{\bar{n}}, A_{\bar{n}}) \sim (q_{\bar{n}}, A_{\bar{n}})$. Since $y^+ \sim l \sim y^-$, it must be

$$(l, b) \sim \frac{1}{P^+} \left(1, \frac{1}{\lambda} \right). \quad (11)$$

Using the projectors defined in Eqs. (A2), (A3), we define the light-cone (LC) good and bad components of the collinear quark field as, respectively,

$$\xi_{\bar{n}} = \Lambda_+ q_{\bar{n}}, \quad (12)$$

$$\eta_{\bar{n}} = \Lambda_- q_{\bar{n}}. \quad (13)$$

From the Dirac equation, we have

$$\eta_{\bar{n}} \sim \lambda \xi_{\bar{n}}, \quad (14)$$

while the gluon field is a vector with natural dimensions of momentum, therefore it scales as its momentum. The \bar{n} -collinear fields do not encode all the nonperturbative physics, hence we also need the v -collinear fields, defined by the scaling relations

$$(\partial^+, \partial^-, \partial_\perp)(q_v, A_v) \lesssim (\lambda^2, \lambda^2, \lambda) P^+(q_v, A_v). \quad (15)$$

The region of small longitudinal momentum is accounted for by both the \bar{n} -collinear and v -collinear fields. Outside the small- x regime, we can assume that hadrons do not contain soft partons, therefore the overlap region reduces to a vacuum contribution, known as the soft factor $S(\{b\})$. Therefore, to remove the double-counting of the overlap region, we can define

$$\tilde{\Omega}_v(y_1, y_2, y_3; P, S) = \int [Dq_{\bar{n}}DA_{\bar{n}}][Dq_vDA_v] e^{iS_{\text{QCD}}[q_{\bar{n}}, A_{\bar{n}}]} e^{iS_{\text{QCD}}[q_v, A_v]} \frac{O_{\text{eff}}(y_1, y_2, y_3)}{S(b_1, b_2, b_3)} \phi(P, S), \quad (16)$$

where

$$O_{\text{eff}}(y_1, y_2, y_3) = \int [D\psi DB] e^{iS_{\text{int}}[\psi, q_{\bar{n}}, q_v, B, A_{\bar{n}}, A_v]} \varepsilon_{ijk} J_{v,i}(y_1) J_{v,j}(y_2) J_{v,k}(y_3), \quad (17)$$

with

$$S_{\text{int}}[\psi, q_{\bar{n}}, q_v, B, A_{\bar{n}}, A_v] = S_{\text{QCD}}[\psi + q_{\bar{n}} + q_v, B + A_{\bar{n}} + A_v] - S_{\text{QCD}}[q_{\bar{n}}, A_{\bar{n}}] - S_{\text{QCD}}[q_v, A_v]. \quad (18)$$

The appropriate soft factor is given by

$$\begin{aligned} S(b_1, b_2, b_3) = & \langle 0 | \frac{1}{3!} \varepsilon_{ijk} [Ln + L_{\perp}, Ln + b_1]_i [Ln + b_1, b_1] [b_1, L\bar{n} + b_1] [L\bar{n} + b_1, L\bar{n} + L_{\perp}]_{i''} \\ & \times [Ln + L_{\perp}, Ln + b_2]_j [Ln + b_2, b_2] [b_2, L\bar{n} + b_2] [L\bar{n} + b_2, L\bar{n} + L_{\perp}]_{j''} \\ & \times [Ln + L_{\perp}, Ln + b_3]_k [Ln + b_3, b_3] [b_3, L\bar{n} + b_3] [L\bar{n} + b_3, L\bar{n} + L_{\perp}]_{k''} \varepsilon_{i''j''k''} |0\rangle, \end{aligned} \quad (19)$$

where we are implying the fundamental-representation color indices contracted through the Wilson lines. It is represented in Fig. 2, and, as we will see in Sec. IV, it compensates the divergences arising from the separation of the \bar{n} -collinear and v -collinear sectors, allowing us to extract the physical three-quark baryon LFWF from the QTMD correlator.

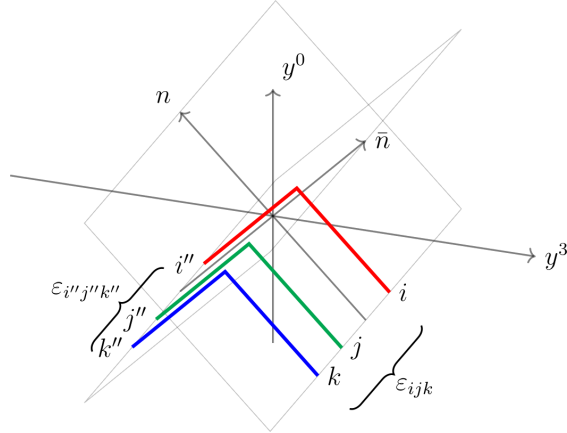


Figure 2. Soft factor for the three-quark baryon LFWF. The lightlike Wilson lines orthogonal to \bar{n} and n connect on the hypersurface $y^3 = 0$. They are colored in red, green and blue to visually indicate the antisymmetrization of the fundamental-representation color indices at both ends. For simplicity, the transverse gauge links at both ends are implied.

Using the scaling relation (11), interactions between volumes around the positions of the quark fields are mediated by propagators of order $b^{-2} \sim (\lambda P^+)^2$. These contributions are not relevant for leading-power (LP) and next-to-leading-power (NLP) calculations. Therefore, the LP and NLP functional integral in Eq. (17) factorizes around the positions of the quarks, i.e.,

$$O_{\text{eff}}(y_1, y_2, y_3) = \varepsilon_{ijk} \mathcal{J}_{v,i}(y_1) \mathcal{J}_{v,j}(y_2) \mathcal{J}_{v,k}(y_3), \quad (20)$$

where we introduced the effective current

$$\mathcal{J}(y) = \int [D\psi DB] e^{iS_{\text{int}}[\psi, q_{\bar{n}}, q_v, B, A_{\bar{n}}, A_v]} J_v(y), \quad (21)$$

with integrals restricted around y .

After integrating over the dynamical fields, the leading-order (LO) contribution is given by tree-level diagrams. To further develop the effective current, it is convenient to fix a gauge. The choice for the background fields can be made independently of that for the dynamical ones: we use the standard Background-Feynman gauge (see Ref. [10]) for the latter, while for the former we choose the LC gauge

$$A_{\bar{n}}^+ = 0, \quad A_v^- = 0. \quad (22)$$

This does not completely fix the gauge, and we use the residual gauge freedom to set to zero the transverse components at infinity, specifically

$$\lim_{z^- \rightarrow \text{sign}(L)\infty} A_{\bar{n},\perp}^\mu(z) = 0, \quad \lim_{z^+ \rightarrow \text{sign}(L)\infty} A_{v,\perp}^\mu(z) = 0. \quad (23)$$

These choices reduce the transverse Wilson lines to the identity, and the remaining gauge links are the identity up to NLP corrections. However, in order to extract the three-quark baryon LFWF in the end, we must keep the representation of the v -collinear sector in terms of the Wilson line

$$P \left[\exp \left(ig \int_0^L d\lambda v_\mu A_v^\mu(\lambda v + y) \right) \right] = H^\dagger(y) = H^\dagger(y_\perp). \quad (24)$$

The last equality holds up to next-to-leading power, after expanding the fields and using the scaling relation (15). Therefore, the LP and LO contribution to the effective current (21) is

$$\mathcal{J}(y) = H^\dagger(y_\perp) \xi_{\bar{n}}(y). \quad (25)$$

In general, we have

$$\mathcal{J}(y) = H^\dagger(y_\perp) \widehat{C}_1 \xi_{\bar{n}}(y), \quad \widehat{C}_1 = I + \mathcal{O}(\alpha_s), \quad (26)$$

where the coefficient functions (CFs) are integral operators acting only on the collinear fields, and I is the identity. The next-to-leading-order (NLO) correction is the contribution of a loop between the quark field and its Wilson line, see Fig. 3.

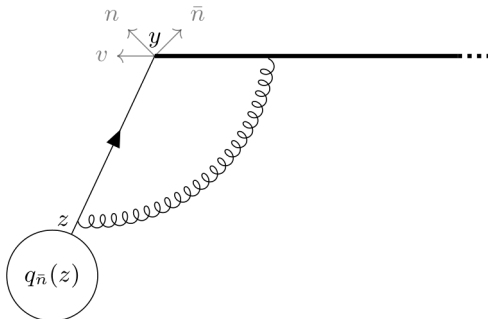


Figure 3. One-loop diagram contributing to the quark current at next-to-leading order. The thick line is the gauge link.

To calculate the NLO effective current (21), we need the explicit expression of the interaction action (18) with two background fields, which can be found in Appendix A of Ref. [11]. We expand a dynamical Wilson line in the current (4) to first order in g , we pick up a $\bar{\psi} B q_{\bar{n}}$ -vertex from S_{int} , and contract the corresponding fields. In $D = 4 - 2\epsilon$ dimensions, this gives

$$ig \int_{y^-}^L d\lambda v^\mu B_\mu(\lambda v + b) \overbrace{\psi(y) ig \int d^D z \bar{\psi} B q_{\bar{n}}(z)} \quad (27)$$

Projecting with Λ_+ as in Eq. (A2) to retain only LP contributions, and using Eqs. (A4)–(A8), we have

$$\widehat{C}_{1,\text{NLO}} \xi_{\bar{n}}(y) = \xi_{\bar{n}}(y) + \frac{ig^2 C_F}{8\pi^D} \Gamma(1 - \epsilon) \Gamma(2 - \epsilon) \int_0^L d\sigma v^\mu \int d^D z \frac{\Lambda_+ (\not{y} - \not{z}) \gamma_\mu \xi_{\bar{n}}(z)}{\left(-(\sigma v + y - z)^2 + i0 \right)^{1-\epsilon} \left(-(y - z)^2 + i0 \right)^{2-\epsilon}}. \quad (28)$$

After integrating, we find (see also Ref. [2])

$$\widehat{C}_{1,\text{NLO}}\xi_{\bar{n}}(y) = 2a_s \left(\frac{-v^2}{4}\right)^\epsilon C_F \frac{1-\epsilon}{1-2\epsilon} \Gamma(-\epsilon) \int_0^L d\tau \frac{(\tau^2)^\epsilon}{\tau} \xi_{\bar{n}}(\tau v^- + y^- + y_\perp). \quad (29)$$

To move to longitudinal momentum space, we Fourier transform lv^- to xP^+ . Since x is the fraction of longitudinal momentum of the baryon carried by an extracted parton, we have $0 \leq x \leq 1$. However, we do the calculations more generally, allowing x to also take negative values, which corresponds to the absorption of an antiparton. Therefore, we have

$$\begin{aligned} & v^- \int dl e^{ilv^- xP^+} 2a_s \left(\frac{-v^2}{4}\right)^\epsilon C_F \frac{1-\epsilon}{1-2\epsilon} \Gamma(-\epsilon) \int_0^L d\tau \frac{(\tau^2)^\epsilon}{\tau} \xi_{\bar{n}}((\tau+l)v^- + b) \\ &= 2a_s \left(\frac{-v^2}{4}\right)^\epsilon C_F \frac{1-\epsilon}{1-2\epsilon} \Gamma(-\epsilon) \left(\int_0^L \frac{d\tau}{\tau} (\tau^2)^\epsilon e^{-i\tau v^- xP^+} \right) \xi_{\bar{n}}(x, b) \\ &= 2a_s C_F \frac{1-\epsilon}{1-2\epsilon} \Gamma(-\epsilon) \Gamma(2\epsilon) \left(\frac{-v^2}{(iss_x 2|x|v^- P^+)^2} \right)^\epsilon \xi_{\bar{n}}(x, b) = C_{1,\text{NLO}}(x) \xi_{\bar{n}}(x, b). \end{aligned} \quad (30)$$

In the first equality, we defined

$$\xi_{\bar{n}}(x, b) = v^- \int dl e^{ilv^- xP^+} \xi_{\bar{n}}(lv^- + b), \quad (31)$$

while in the second equality we defined $s = \text{sign}(L)$, $s_x = \text{sign}(x)$. Technically, in Eq. (31) we still have to respect $|l| \ll |L|$, which implies $|x| \gg |LP^+|^{-1}$. This condition is compatible with the assumption of being outside the small- x regime.

III. FACTORIZATION OF THE QTMD CORRELATOR

We can now show how the three-quark baryon LFWFs emerges from the QTMD correlator (3). Inserting back the effective quark currents (26) into Eq. (16), and assuming that the hadron is made up of collinear partons only, the path integrals for the \bar{n} -collinear and the v -collinear sectors factorize from each other. In a gauge-invariant formulation, and requiring the matrix elements to remain color neutral, we have

$$\widetilde{\Omega}_v(y_1, y_2, y_3; P, S) = \frac{\Psi(b_1, b_2, b_3) \widehat{C}_1 \widehat{C}_1 \widehat{C}_1 \widetilde{\Phi}_{111}(\{y_q\}_{q=1,2,3}; P, S)}{S(b_1, b_2, b_3)}, \quad (32)$$

where $y_q = y_q^- n + b_q$, with b_q purely transverse. Here, $\widetilde{\Phi}_{111}$ is exactly the LP three-quark baryon LFWF in position space, Ψ is a lattice factor, and S is the soft factor (19).

For the LFWF, we have

$$\begin{aligned} \widetilde{\Phi}_{111}(\{y_q\}; P, S) &= \langle 0 | \varepsilon_{ijk} [Ln + \infty_\perp, Ln + b_1]_{\bar{n}, ii'} [Ln + b_1, y_1^- n + b_1]_{\bar{n}, i' i''} \xi_{\bar{n}, i''}(y_1^- n + b_1) \\ &\quad \times [Ln + \infty_\perp, Ln + b_2]_{\bar{n}, jj'} [Ln + b_2, y_2^- n + b_2]_{\bar{n}, j' j''} \xi_{\bar{n}, j''}(y_2^- n + b_2) \\ &\quad \times [Ln + \infty_\perp, Ln + b_3]_{\bar{n}, kk'} [Ln + b_3, y_3^- n + b_3]_{\bar{n}, k' k''} \xi_{\bar{n}, k''}(y_3^- n + b_3) | P, S \rangle, \end{aligned} \quad (33)$$

where we summed over color indices in the fundamental representation. The n -directed Wilson lines are defined as

$$[Ln + b_q, y_q^- n + b_q]_{\bar{n}} = P \left[\exp \left(ig \int_{y_q^-}^L d\sigma n^\mu A_{\bar{n}, \mu}(\sigma n + b_q) \right) \right], \quad (34)$$

where $L = -\infty, +\infty$ for an hadron in the initial or final state, respectively, and analogously for the gauge links to transverse infinity. The first CF \widehat{C}_1 in Eq. (32) acts on the first quark operator, and so on.

For the lattice factor, we have

$$\Psi(b_1, b_2, b_3) = \langle 0 | \frac{1}{3!} \varepsilon_{ijk} H_i^\dagger(b_1) [b_1, L\bar{n} + b_1]_v [L\bar{n} + b_1, L\bar{n} + \infty_\perp]_{v, i''} \rangle$$

$$\begin{aligned}
& \times H_j^\dagger(b_2) [b_2, L\bar{n} + b_2]_v [L\bar{n} + b_2, L\bar{n} + \infty_\perp]_{v,j''} \\
& \times H_k^\dagger(b_3) [b_3, L\bar{n} + b_3]_v [L\bar{n} + b_3, L\bar{n} + \infty_\perp]_{v,k''} \varepsilon_{i''j''k''} |0\rangle,
\end{aligned} \tag{35}$$

where H^\dagger is defined in Eq. (24), while the transverse and \bar{n} -directed Wilson lines are defined analogously to Eq. (34), with the replacement $A_{\bar{n}} \mapsto A_v$. Throughout, we implicitly contract the fundamental-representation color indices through the Wilson lines.

The LFWF and the lattice factor are represented in Figs. 4 and 5, respectively.

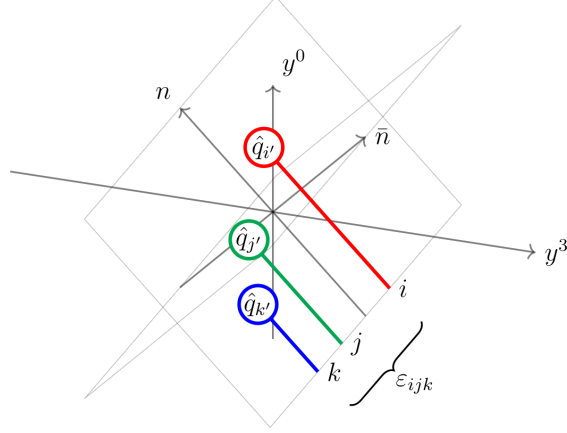


Figure 4. Leading-power baryon three-quark LFWF. The quark fields lie on the hypersurface tangent to the light cone and orthogonal to \bar{n} . The lightlike Wilson lines are colored in red, green and blue to visually indicate the antisymmetrization of the fundamental-representation color indices. For simplicity, the transverse gauge links are implied.

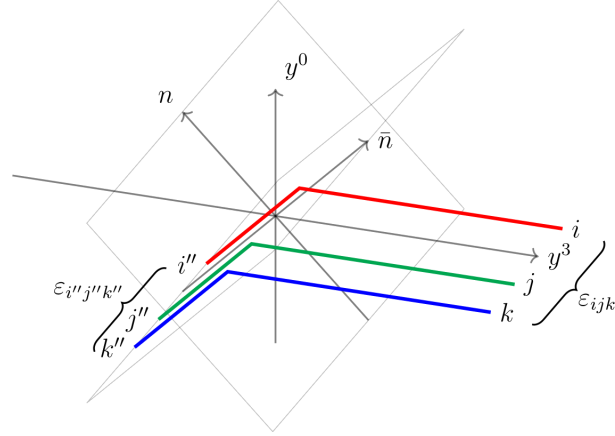


Figure 5. Lattice factor for the baryon three-quark LFWF. The lightlike and v -directed Wilson lines connect on the hypersurface $y^3 = 0$. They are colored in red, green and blue to visually indicate the antisymmetrization of the fundamental-representation color indices on both ends. For simplicity, the transverse gauge links on both ends are implied.

From Eq. (30), in longitudinal-momentum-fraction space we have

$$\Omega_v(\{x_q, b_q\}_{q=1,2,3}; P, S) = \frac{\Psi(\{b_q\}) C_1(x_1) C_1(x_2) C_1(x_3) \Phi_{111}(\{x_q, b_q\}; P, S)}{S(\{b_q\})} \delta(x_1 + x_2 + x_3 - 1), \tag{36}$$

where

$$\Phi_{111}(\{x_q, b_q\}) = \int dy_1^- dy_2^- dy_3^- e^{iP^+ \sum_q y_q^- x_q} \tilde{\Phi}_{111}(\{y_q^-, b_q\}). \tag{37}$$

The x_q are the fractions of longitudinal momentum of the baryon carried by the quarks, therefore, by momentum conservation, we must have $\sum_q x_q = 1$.

Going beyond leading order, we encounter an interconnected structure of divergences. Alongside ultraviolet (UV) and infrared (IR) divergences, we have rapidity divergences, when a lightlike component of a loop momentum k goes to infinity at constant k^2 . The UV and IR divergences are regulated using dimensional regularization in $D = 4 - 2\epsilon$ dimensions, while rapidity divergences we handled using δ -regularization, i.e.,

$$[Ln + z, z] \mapsto P \left[\exp \left(ig \int_0^L d\sigma n^\mu A_\mu(\sigma n + z) e^{-|\sigma|\delta^+} \right) \right], \quad (38)$$

$$[z, L\bar{n} + z] \mapsto P \left[\exp \left(ig \int_L^0 d\eta \bar{n}^\mu A_\mu(\eta \bar{n} + z) e^{-|\eta|\delta^-} \right) \right], \quad (39)$$

where $\delta^\pm > 0$ have dimensions of mass, and we define $\delta^2 = 2\delta^+\delta^-$. Rapidity divergences are multiplicatively renormalizable, as we will see explicitly at next-to-leading order, after regularization and the introduction of momentum scales ν_q^+, ν_q^- for each quark and for direction n, \bar{n} , respectively, with $\nu_q^2 = 2\nu_q^+\nu_q^-$.

The divergences from the factorization procedure must recombine so that only the ones of the original QTMD correlator remain, and, up to next-to-leading power, all divergences must cancel independently for each leg. Moreover, in order to extract a physical LFWF, it must be renormalizable independently of the lattice factor. We will prove all this in the following section, while in the remainder of this section we calculate all the divergent contributions, working in momentum space and choosing the $\overline{\text{MS}}$ renormalization scheme. Note that the calculations proceed identically for any number of colors N , provided we consider N -point operators. To avoid unnecessary notational clutter, we focus on the three-quark case of primary interest, but we evaluate the color structures for generic N once and for all.

A. Divergences of the Light-Front Wave Function

We start by calculating the divergences of the three-quark LFWF (33) at next-to-leading order. They come from one-loop interactions between a quark and a lightlike Wilson line, either the one directly connected to it, or the gauge link associated to another quark.

We first consider the divergences originating from interactions with a transverse separation, diagrammatically represented in Fig. 6.

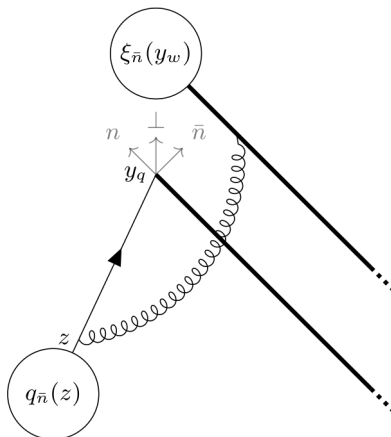


Figure 6. One-loop diagram for the interaction between a quark and a n -directed Wilson line at different transverse positions.

Going back to the TMD expansion with two background fields, and once again choosing the standard Feynman gauge for dynamical fields and the LC gauge (22), (23) for the background fields, we can construct the contributions from the analogous of the contraction in (27). For, e.g., quark 1 interacting with the Wilson line of quark 2, we have to consider the contraction

$$\varepsilon_{ijk} \delta_{ii'} \delta_{kk'} ig \int_{y_2^-}^L d\sigma n^\mu B_{\mu, jj'}(\sigma n + b_2) \overbrace{\psi_{i'}(y_1) ig \int d^D z \bar{\psi} \not{B} q_{\bar{n}}(z) \xi_{\bar{n}, j'}(y_2) \xi_{\bar{n}, k'}} \quad (40)$$

where $\delta_{ii'}$ and $\delta_{kk'}$ come from the order-zero expansions of the dynamical Wilson lines for quark 1 and quark 3. Using

Eqs. (A4), (A5), for the color structure we have

$$\varepsilon_{ijk} \left(\sum_{A=1}^{N^2-1} t_{jj'}^A t_{il}^A \right) q_{\bar{n},l}(z) \xi_{\bar{n},j'}(y_2) \xi_{\bar{n},k}(y_3) = -\frac{C_F}{N-1} \varepsilon_{ijk} q_{\bar{n},i}(z) \xi_{\bar{n},j}(y_2) \xi_{\bar{n},k}(y_3), \quad (41)$$

where we used Eq. (A6), and C_F is defined in Eq. (A7). Projecting with Λ_+ as in Eq. (A2) to retain only LP contributions, we have

$$\text{diag}_{12} = \frac{ig^2}{8\pi^D} \frac{C_F}{N-1} \Gamma(1-\epsilon) \Gamma(2-\epsilon) \int_{y_2^-}^L d\sigma \int d^D z \varepsilon_{ijk} \frac{\Lambda_+ (y_1^- \gamma^+ + b_1' - \not{z}) \gamma^+ q_{\bar{n},i}(z) \xi_{\bar{n},j}(y_2) \xi_{\bar{n},k}(y_3)}{(-(\sigma n + b_2 - z)^2 + i0)^{1-\epsilon} \left(-(y_1^- n + b_1 - z)^2 + i0 \right)^{2-\epsilon}}. \quad (42)$$

After integrating, and keeping only the rapidity divergent part, we find

$$\text{diag}_{12} = -2a_s \frac{C_F}{N-1} \Gamma(-\epsilon) \left(\frac{-b_{21}^2}{4} \right)^\epsilon \ln \frac{\delta^+}{i s \hat{p}_1^+} \varepsilon_{ijk} \xi_{\bar{n},i}(y_1) \xi_{\bar{n},j}(y_2) \xi_{\bar{n},k}(y_3) + \dots, \quad (43)$$

where the ellipsis represent rapidity-finite terms. Note that this contribution, as well as all the other rapidity-finite terms not explicitly considered, are also IR divergent, as evident from the factor of $\Gamma(-\epsilon)$. These divergences can be ignored for the purpose of studying the scale evolution of the LFWF, therefore we also remove the pole at $\epsilon = 0$ from Eq. (43). The contributions from quark 2 interacting with the Wilson line of quark 1, and all other combinations, are calculated in exactly the same way. Therefore, the total NLO rapidity-divergent contribution is

$$\sum_{\substack{q,w=1 \\ w \neq q}}^N \text{diag}_{qw} = -2a_s \frac{C_F}{N-1} \sum_{\substack{q,w=1 \\ w \neq q}}^N \left(\Gamma(-\epsilon) \left(\frac{-(b_w - b_q)^2}{4} \right)^\epsilon + \frac{1}{\epsilon} \right) \ln \left(\frac{\delta^+}{i \text{sign}(L) \hat{p}_q^+} \right) \varepsilon_{ijk} \xi_{\bar{n},i}(y_1) \xi_{\bar{n},j}(y_2) \xi_{\bar{n},k}(y_3). \quad (44)$$

Next, we consider the NLO contributions from a gluon exchange between a quark and the corresponding Wilson line, diagrammatically represented in Fig 7.

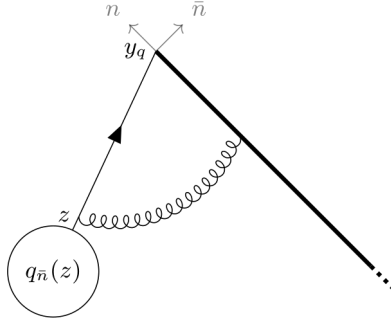


Figure 7. One-loop diagram for the interaction between a quark and a n -directed Wilson line at the same transverse position.

The integral to be evaluated is analogous to the case with transverse separation, but its absence makes it UV divergent. The calculation proceeds in a similar fashion to the previous one, but it generates a different color structure. Considering, e.g., quark 1, we have

$$\varepsilon_{ijk} \left(\sum_{A=1}^{N^2-1} t_{ii'}^A t_{i'l}^A \right) q_{\bar{n},l}(z) \xi_{\bar{n},j}(y_2) \xi_{\bar{n},k}(y_3) = C_F \varepsilon_{ijk} q_{\bar{n},i}(z) \xi_{\bar{n},j}(y_2) \xi_{\bar{n},k}(y_3). \quad (45)$$

Adapting Eq. (43), we find

$$\text{diag}_{11} = +2a_s C_F \Gamma(\epsilon) \left(1 + \ln \left(\frac{\delta^+}{i \text{sign}(L) \hat{p}_1^+} \right) \right) \varepsilon_{ijk} \xi_{\bar{n},i}(y_1) \xi_{\bar{n},j}(y_2) \xi_{\bar{n},k}(y_3), \quad (46)$$

where δ^+ now regularizes the collinear divergences from the interaction with the Wilson line at infinity. These are conceptually different from rapidity divergences, since they do not depend on the transverse separation. The calculations proceed identically for each quark, therefore we can extract the UV renormalization constant for the LP field

up to next-to-leading order. In momentum space, and in the $\overline{\text{MS}}$ renormalization scheme, we have

$$\begin{aligned}\tilde{Z}_{U1;\overline{\text{MS}}}\left(\frac{\delta^+}{p_q^+}\right) &= 1 + 2a_s C_F \Gamma(\epsilon) e^{\epsilon\gamma_E} (\mu^2)^\epsilon \left(1 + \ln\left(\frac{\delta^+}{i\text{sign}(L) p_q^+}\right)\right) + \mathcal{O}(a_s^2) \\ &= 1 + 2a_s C_F \frac{1}{\epsilon} \left(1 + \ln\left(\frac{\delta^+}{i\text{sign}(L) p_q^+}\right)\right) + \mathcal{O}(a_s^2),\end{aligned}\quad (47)$$

where p_q^+ is the longitudinal momentum of quark q , and in the second equality we expanded around $\epsilon = 0$. Incorporating the quark self-energy, i.e. [11],

$$Z_{2;\overline{\text{MS}}}^{\frac{1}{2}} = 1 - a_s C_F \frac{1}{2\epsilon} + \mathcal{O}(a_s^2), \quad (48)$$

we have

$$Z_{U1;\overline{\text{MS}}}\left(\frac{\delta^+}{p_q^+}\right) = 1 + a_s C_F \frac{1}{\epsilon} \left(\frac{3}{2} + 2 \ln\left(\frac{\delta^+}{i\text{sign}(L) p_q^+}\right)\right) + \mathcal{O}(a_s^2). \quad (49)$$

Note that the self-energy of an n -directed Wilson line is zero, since it is calculated from the contraction of two terms $\sim n^\mu B_\mu$, and therefore it is proportional to $n^2 = 0$.

By moving to momentum space and introducing momentum scales ν_q^+ , we extract from Eq. (44) the correction from rapidity divergences to the LP LFWF up to next-to-leading order. In the $\overline{\text{MS}}$ scheme, we have

$$R_{\overline{\text{MS}}}(\delta^+, \{\nu_q^+\}) = \prod_{q=1}^N R_{\overline{\text{MS}}}\left(\frac{\delta^+}{\nu_q^+}\right), \quad (50)$$

where the correction from each quark is given by

$$R_{\overline{\text{MS}}}\left(\frac{\delta^+}{\nu_q^+}\right) = 1 + 2a_s \frac{C_F}{N-1} \sum_{\substack{w=1 \\ w \neq q}}^N \ln\left(\frac{-(b_w - b_q)^2}{4} \mu^2\right) \ln\left(\frac{\delta^+}{\nu_q^+}\right) + \mathcal{O}(a_s^2). \quad (51)$$

Note that we dropped terms $\sim \ln(-\mu^2 (b_w - b_q)^2 / 4) \ln(\nu_q^+ / p_q^+)$, since they are not divergent.

The results are equivalent to those for TMD parton distribution functions and fragmentation functions in Ref. [11], taking into account the different color structure, and the fact that our Wilson lines always extend toward infinity. Since there is no contraction between Dirac adjoints, the imaginary parts of the renormalization constants do not compensate, and therefore we kept their contribution in Eq. (49).

Analogous results would be found in any gauge. In a gauge-invariant formulation, alongside the contraction (40), we would have to consider all other terms in the expansion of the Wilson line with exactly one dynamical field, as well as the terms in the remaining two links with no dynamical fields. Ultimately, we are left with the gauge links in the background. Two quarks are connected to the Levi-Civita symbol through their background Wilson lines, allowing us to directly adapt the procedure used previously. To understand how we recover the last background link, consider, e.g., the three contractions from the $\mathcal{O}(g^3)$ -expansion, using only a single type of background field for simplicity. We have

$$\begin{aligned}& + \int_a^b dx_1 A(x_1) \int_{x_1}^b dx_2 A(x_2) \int_{x_2}^b dx_3 B(x_3) + \int_a^b dx_1 A(x_1) \int_{x_1}^b dx_2 B(x_2) \int_{x_2}^b dx_3 A(x_3) \\ & + \int_a^b dx_1 B(x_1) \int_{x_1}^b dx_2 A(x_2) \int_{x_2}^b dx_3 A(x_3) \\ = & + \int_a^b dx_1 A(x_1) \int_{x_1}^b dx_2 A(x_2) \int_{x_2}^b dx_3 B(x_3) + \int_a^b dx_1 A(x_1) \int_{x_1}^b dx_3 A(x_3) \int_{x_1}^{x_3} dx_2 B(x_2) \\ & + \int_a^b dx_2 A(x_2) \int_a^{x_2} dx_1 B(x_1) \int_{x_2}^b dx_3 A(x_3) \\ = & + \int_a^b dx_1 A(x_1) \int_{x_1}^b dx_2 A(x_2) \int_{x_2}^b dx_3 B(x_3) + \int_a^b dx_1 A(x_1) \int_{x_1}^b dx_2 A(x_2) \int_{x_1}^{x_2} dx_3 B(x_3)\end{aligned}$$

$$\begin{aligned}
& + \int_a^b dx_1 A(x_1) \int_a^{x_1} dx_3 B(x_3) \int_{x_1}^b dx_2 A(x_2) \\
= & + \int_a^b dx_1 A(x_1) \int_{x_1}^b dx_2 A(x_2) \int_a^b dx_3 B(x_3),
\end{aligned} \tag{52}$$

where in the second equality we renamed the integration variables so that $x_2 \leftrightarrow x_3$ in the second term, and $x_2 \rightarrow x_1 \rightarrow x_3 \rightarrow x_2$ in the third term. Considering all terms in the expansion of the Wilson line with one dynamical field, we recover that the exchanged gluon can attach to any point along the path of the gauge link, while the last quark remains connected to the Levi-Civita symbol through a background Wilson line.

B. Divergences of the Lattice Factor

We now turn to the NLO divergent contributions to the lattice factor (35), which come from one-gluon exchanges between a v -directed and a \bar{n} -directed Wilson line.

First, we consider the divergences originating from gluon exchanges with a transverse separation, diagrammatically represented in Fig. 8.

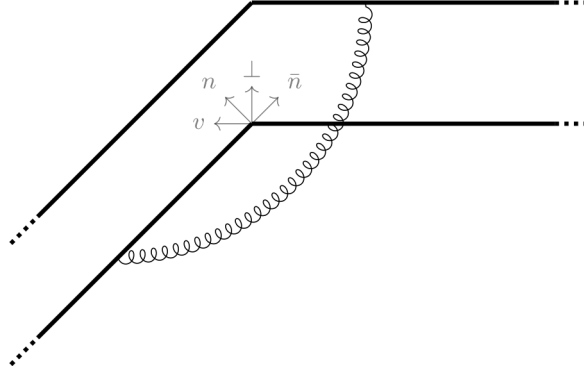


Figure 8. One-loop diagram for a gluon exchange between a v and a \bar{n} -directed Wilson line at different transverse positions.

For, e.g., gauge links at b_1 and b_2 , we have to consider the contraction

$$\varepsilon_{ijk} \delta_{ii'} \delta_{kk'} ig \int_0^L d\lambda v^\mu B_{\mu, i' i''}(\lambda v + b_1) ig \int_L^0 d\eta \bar{n}^\nu B_{\nu, j j'}(\eta \bar{n} + b_2) \delta_{j' j''} \varepsilon_{i'' j'' k'}, \tag{53}$$

where the Kronecker delta come from the order-zero expansions of the remaining Wilson lines. Using Eq. (A5), for the color structure we have

$$\frac{1}{N!} \varepsilon_{ijk} \left(\sum_{A=1}^{N^2-1} t_{ii'}^A t_{jj''}^A \right) \varepsilon_{i'' j'' k} = -\frac{C_F}{N-1}, \tag{54}$$

where we used Eq. (A6). Therefore, defining $s = \text{sign}(L)$ and including δ -regularization, we have

$$\text{diag}'_{12} = -\frac{g^2}{4\pi^{2-\epsilon}} \frac{C_F}{N-1} \Gamma(1-\epsilon) \int_0^L d\lambda \int_L^0 d\eta v \bar{n} e^{-\delta^- s \eta} \frac{1}{\left(-(\lambda v + b_1 - \eta \bar{n} - b_2)^2 + i0 \right)^{1-\epsilon}} \Psi. \tag{55}$$

Similarly to the LFWF, we isolate the rapidity divergent contributions, alongside those from the other combinations of Wilson lines. The total NLO contribution from diagrams with transverse separation is

$$\sum_{\substack{q, w=1 \\ w \neq q}}^N \text{diag}'_{qw} = +2a_s C_F \sum_{q=1}^N \Gamma(1-2\epsilon) \Gamma(2\epsilon) \Gamma(\epsilon) \left(\frac{\text{sign}(L) \sqrt{-v^2 \delta^-}}{v^-} \right)^{-2\epsilon} \Psi$$

$$-a_s \frac{C_F}{N-1} \sum_{\substack{q,w=1 \\ w \neq q}}^N \Gamma(-\epsilon) \left(\frac{-(b_q - b_w)^2}{4} \right)^\epsilon \left(-\psi(-\epsilon) - \gamma_E + \ln \left(\frac{-(b_q - b_w)^2}{4} (-v^2) \left(\frac{\delta^-}{v^-} \right)^2 \right) \right) \Psi, \quad (56)$$

where ψ is the Digamma function, i.e., $\psi(z) = (\Gamma'/\Gamma)(z)$.

Next, we consider the NLO contributions from a gluon exchange between a v -directed Wilson line and the corresponding lightlike link, diagrammatically represented in Fig. 9.

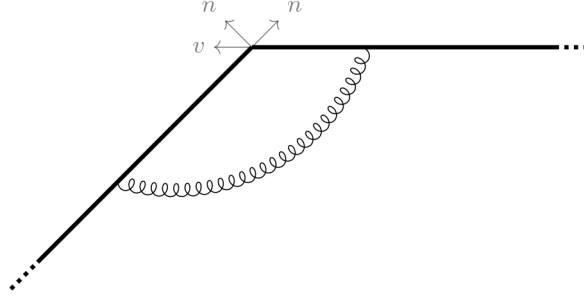


Figure 9. One-loop diagram for a gluon exchange between a v and a \bar{n} -directed Wilson line at the same transverse position.

The calculations are analogous to the case with transverse separation. The only difference is in the color structure, e.g., for the Wilson lines at b_1 we have

$$\frac{1}{N!} \varepsilon_{ijk} \delta_{jj'} \delta_{kk'} \left(\sum_{A=1}^{N^2-1} t_{ii'}^A t_{i'i''}^A \right) \varepsilon_{i''j''k''} = C_F. \quad (57)$$

Adapting Eq. (56), for the total NLO contribution from diagrams with zero transverse separation we find

$$\sum_{q=1}^N \text{diag}'_{qq} = -2a_s C_F \sum_{q=1}^N \Gamma(1-2\epsilon) \Gamma(2\epsilon) \Gamma(\epsilon) \left(\frac{\text{sign}(L) \sqrt{-v^2} \delta^-}{v^-} \right)^{-2\epsilon} \Psi. \quad (58)$$

Adding up Eqs. (56) and (58), there is a compensation between the latter and the first term of the former. The same cancellation occurs for each leg of the lattice factor. Therefore, the total divergent correction in the $\overline{\text{MS}}$ renormalization scheme up to next-to-leading order is

$$\begin{aligned} \tilde{\Delta}_{\Psi; \overline{\text{MS}}} &= 1 - a_s \frac{C_F}{N-1} \sum_{\substack{q,w=1 \\ w \neq q}}^N \Gamma(-\epsilon) e^{-\epsilon \gamma_E} \left(\frac{-(b_q - b_w)^2 \mu^2}{4} \right)^\epsilon \left(-\psi(-\epsilon) - \gamma_E + \ln \left(\frac{-(b_q - b_w)^2}{4} (-v^2) \left(\frac{\delta^-}{v^-} \right)^2 \right) \right) \\ &\quad + \mathcal{O}(a_s^2) \\ &= 1 - N a_s C_F \left(\frac{1}{\epsilon^2} - \frac{1}{\epsilon} \ln \left(\frac{\sqrt{-v^2} \delta^-}{\mu v^-} \right)^2 \right) + 2a_s \frac{C_F}{N-1} \sum_{\substack{q,w=1 \\ w \neq q}}^N \left(\frac{1}{\epsilon} + \ln \left(\frac{-(b_q - b_w)^2 \mu^2}{4} \right) \right) \ln \left(\frac{\delta^-}{\nu_q^-} \right) + \mathcal{O}(a_s^2) \\ &= \tilde{Z}_{\Psi 1; \overline{\text{MS}}}^N \left(\frac{\sqrt{-v^2} \delta^-}{\mu v^-} \right) R_{\overline{\text{MS}}}(\delta^-, \{\nu_q^-\}). \end{aligned} \quad (59)$$

In the second equality, we introduced the momentum scales ν_q^- , and kept only divergent terms. In the last equality, we defined the renormalization constant

$$\tilde{Z}_{\Psi 1; \overline{\text{MS}}} \left(\frac{\sqrt{-v^2} \delta^-}{\mu v^-} \right) = 1 - a_s C_F \left(\frac{1}{\epsilon^2} - \frac{1}{\epsilon} \ln \left(\frac{\sqrt{-v^2} \delta^-}{\mu v^-} \right)^2 \right) + \mathcal{O}(a_s^2), \quad (60)$$

and the correction from rapidity divergences

$$R_{\overline{\text{MS}}}(\delta^-, \{\nu_q^-\}) = \prod_{q=1}^N R_{\overline{\text{MS}}}\left(\frac{\delta^-}{\nu_q^-}\right), \quad (61)$$

with

$$R_{\overline{\text{MS}}}\left(\frac{\delta^-}{\nu_q^-}\right) = 1 + 2a_s \frac{C_F}{N-1} \sum_{\substack{w=1 \\ w \neq q}}^N \ln\left(\frac{-(b_q - b_w)^2}{4} \mu^2\right) \ln\left(\frac{\delta^-}{\nu_q^-}\right) + \mathcal{O}(a_s^2). \quad (62)$$

To get the full renormalization constant, we need to add the self-energy contributions of the Wilson lines, which come from contracting the second-order terms in the expansion of the path-ordered exponentials. For v -directed links, in the $\overline{\text{MS}}$ renormalization scheme and explicitly up to next-to-leading order, we have [2]

$$Z_{H;\overline{\text{MS}}}^{\frac{1}{2}} = 1 + a_s C_F \frac{1}{\epsilon} + \mathcal{O}(a_s^2), \quad (63)$$

Note that there are also IR divergences from the limit $L \rightarrow \pm\infty$, which we collectively encode in a renormalization constant Z_W (see also Eq. (75)). These divergences come directly from the QTMD correlator, and cancel out in Eqs. (32), (36). Since $\bar{n}^2 = 0$, the self-energy of the lightlike link is zero, and therefore the full renormalization constant is

$$Z_{\Psi_1;\overline{\text{MS}}}\left(\frac{\sqrt{-v^2}\delta^-}{\mu v^-}\right) = 1 - a_s C_F \left(\frac{1}{\epsilon^2} - \frac{1}{\epsilon} - \frac{1}{\epsilon} \ln\left(\frac{\sqrt{-v^2}\delta^-}{\mu v^-}\right)^2\right) + \mathcal{O}(a_s^2). \quad (64)$$

C. Factorization of the Soft Factor

At LO, the soft factor (19) reduces to the identity, and we conclude the section by demonstrating a fully factorized structure at next-to-leading order. The NLO corrections are computed in complete analogy with the lattice factor, yielding

$$S_{\text{NLO}}(\{b\}; \delta^+, \delta^-) = -2a_s \frac{C_F}{N-1} \sum_{\substack{q,w=1 \\ w \neq q}}^N \Gamma(-\epsilon) \left(\frac{-(b_q - b_w)^2}{4}\right)^\epsilon \left(-\psi(-\epsilon) - \gamma_E + \ln\left(\frac{-(b_q - b_w)^2}{4} 2\delta^+ \delta^-\right)\right). \quad (65)$$

Note that the rapidity-divergent term is linear in $\ln \delta^+ \delta^-$, therefore we can separate the contributions from n -directed and \bar{n} -directed Wilson lines.

In the $\overline{\text{MS}}$ renormalization scheme and explicitly up to next-to-leading order, we have

$$\begin{aligned} S_{\overline{\text{MS}}}(\{b\}; \delta^2) &= 1 - 2a_s \frac{C_F}{N-1} \sum_{\substack{q,w=1 \\ w \neq q}}^N \left(\frac{1}{\epsilon^2} - \left(\frac{1}{\epsilon} + \ln\left(\frac{-(b_q - b_w)^2}{4} \mu^2\right)\right)\right) \ln\left(\frac{2\delta^+ \delta^-}{\mu^2}\right) \\ &\quad - \frac{1}{2} \ln^2\left(\frac{-(b_q - b_w)^2}{4} \mu^2\right) - \frac{\pi^2}{12} + \mathcal{O}(a_s^2). \end{aligned} \quad (66)$$

Introducing the momentum scales ν_q^\pm , we can isolate the rapidity-divergent contributions associated with n -directed and \bar{n} -directed Wilson lines, i.e.,

$$R_{\overline{\text{MS}}}(\delta^\pm, \{\nu_q^\pm\}) = \prod_{q=1}^N R_{\overline{\text{MS}}}\left(\frac{\delta^\pm}{\nu_q^\pm}\right), \quad (67)$$

with

$$R_{\overline{\text{MS}}}\left(\frac{\delta^\pm}{\nu_q^\pm}\right) = 1 + 2a_s \frac{C_F}{N-1} \sum_{\substack{w=1 \\ w \neq q}}^N \ln\left(\frac{-(b_q - b_w)^2}{4} \mu^2\right) \ln\left(\frac{\delta^\pm}{\nu_q^\pm}\right) + \mathcal{O}(a_s^2). \quad (68)$$

Similarly, the renormalization constants associated with collinear divergences are

$$Z_{R;\overline{\text{MS}}}(\delta^\pm, \{\nu_q^\pm\}) = \prod_{q=1}^N Z_{R;\overline{\text{MS}}}\left(\frac{\delta^\pm}{\nu_q^\pm}\right). \quad (69)$$

with

$$Z_{R;\overline{\text{MS}}}\left(\frac{\delta^\pm}{\nu_q^\pm}\right) = 1 + 2a_s C_F \frac{1}{\epsilon} \ln\left(\frac{\delta^\pm}{\nu_q^\pm}\right) + \mathcal{O}(a_s^2). \quad (70)$$

The UV-divergent part is

$$Z_{S;\overline{\text{MS}}}(\{\nu_q^2\}) = \prod_{q=1}^N Z_{S;\overline{\text{MS}}}(\nu_q^2), \quad (71)$$

with

$$Z_{S;\overline{\text{MS}}}(\nu_q^2) = 1 - 2a_s C_F \left(\frac{1}{\epsilon^2} - \frac{1}{\epsilon} \ln\left(\frac{\nu_q^2}{\mu^2}\right) \right) + \mathcal{O}(a_s^2). \quad (72)$$

The remaining finite part is

$$S_{0;\overline{\text{MS}}}(\{\nu_q^2\}) = 1 + 2a_s \frac{C_F}{N-1} \sum_{\substack{q,w=1 \\ w \neq q}}^N \ln\left(\frac{-(b_q - b_w)^2}{4} \mu^2\right) \ln\left(\frac{\nu_q^2}{\mu^2}\right) + \frac{1}{2} \ln^2\left(\frac{-(b_q - b_w)^2}{4} \mu^2\right) + \frac{\pi^2}{12} + \mathcal{O}(a_s^2). \quad (73)$$

With the quantities introduced in Eqs. (67)–(73), we can express the soft factor in a completely factorized form, i.e.,

$$\begin{aligned} S_{\overline{\text{MS}}}(\delta^2) &= \left(\prod_{c=\pm} R_{\overline{\text{MS}}}(\delta^c, \{\nu_q^c\}) Z_{R;\overline{\text{MS}}}(\delta^c, \{\nu_q^c\}) \right) Z_{S;\overline{\text{MS}}}(\{\nu_q^2\}) S_{0;\overline{\text{MS}}}(\{\nu_q^2\}) \\ &= R_{\overline{\text{MS}}}(\delta^+, \{\nu_q^+\}) R_{\overline{\text{MS}}}(\delta^-, \{\nu_q^-\}) Z_{S;\overline{\text{MS}}}^N(\delta^2) S_{0;\overline{\text{MS}}}(\{\nu_q^2\}). \end{aligned} \quad (74)$$

IV. CANCELLATION OF DIVERGENCES AND PHYSICAL LIGHT-FRONT WAVE FUNCTION

We collect the results from the previous sections to verify, at next-to-leading order, the cancellation of divergences from the factorization of the QTMD correlator. The result will be a well-defined physical LFWF, independently of the residual lattice factor.

From now on, we will explicitly distinguish bare quantities from their renormalized counterparts. For the QTMD correlator, we have

$$\Omega_{v,\text{bare}}(\{x_q, b_q\}; P, S) = Z_W Z_J^3 \Omega_v(\{x_q, b_q\}, \mu, L; P, S), \quad (75)$$

where Z_W renormalizes the v -directed Wilson lines close to infinity, and each Z_J renormalizes a remaining semicompact operator (4). The same factor Z_W appears in the renormalization of the lattice factor, and therefore cancels in Eqs. (32), (36) (see also discussion after Eq. (63)). On the other hand, we have

$$\begin{aligned} & \frac{\Psi_{\text{bare}}(\{b_q\}) C_1(x_1) C_1(x_2) C_1(x_3) \Phi_{111,\text{bare}}(\{x_q, b_q\})}{S(\{b_q\})} \\ &= \frac{R(\delta^-, \{\nu_q^-\}) Z_{\Psi 1}^N \left(\frac{\sqrt{-v^2} \delta^-}{\mu v^-} \right) R(\delta^+, \{\nu_q^+\}) \left(\prod_{q=1}^N Z_{U 1} \left(\frac{\delta^+}{p_q^+} \right) \right)}{R(\delta^+, \{\nu_q^+\}) Z_R(\delta^+, \{\nu_q^+\}) R(\delta^-, \{\nu_q^-\}) Z_R(\delta^-, \{\nu_q^-\}) Z_S(\{\nu_q^2\})} \\ & \times \frac{\Psi(\{b_q\}, \mu, \{\nu_q^-\}) C_1(x_1) C_1(x_2) C_1(x_3) \Phi_{111}(\{x_q, b_q\}, \mu, \{\nu_q^+\})}{S_0(\{\nu_q^2\})}, \end{aligned} \quad (76)$$

where, in the $\overline{\text{MS}}$ renormalization scheme, the divergences of the lattice factor are given by Eqs. (61), (64), while those of the LFWF are given by Eqs. (50), (49), and we used the factorized form (74) of the soft factor. Comparing the

rapidity-divergent contributions in the numerator with those of the soft factor in Eq. (67), we see that they cancel out exactly, thus justifying the use of the same notation. The collinear divergences in each Z_{Ψ_1}, Z_{U_1} are instead canceled out by the corresponding renormalization factor (70), which trades the dependence on δ^\pm for ν_q^\pm . As a result, we are left with

$$\begin{aligned}
& \frac{\prod_{q=1}^N Z_{\Psi_1}\left(\frac{\sqrt{-v^2}\nu_q^-}{\mu v^-}\right) Z_{U_1}\left(\frac{\nu_q^+}{p_q^+}\right) \Psi C_1(x_1) C_1(x_2) C_1(x_3) \Phi_{111}}{Z_S(\{\nu_q^2\}) S_0(\{\nu_q^2\})} \\
&= \left(\prod_{q=1}^N \frac{Z_{U_1}\left(\frac{\nu_q^+}{p_q^+}\right) Z_{\Psi_1}\left(\frac{\sqrt{-v^2}\nu_q^-}{\mu v^-}\right)}{Z_S^{\frac{1}{2}}(\nu_q^2)} \right) C_1(x_1) C_1(x_2) C_1(x_3) \frac{\Phi_{111}}{S_0^{\frac{1}{2}}(\{\nu_q^2\})} \frac{\Psi}{S_0^{\frac{1}{2}}(\{\nu_q^2\})} \\
&= \left(\prod_{q=1}^N Z_{U_1,\text{sub}} Z_{\Psi_1,\text{sub}} \right) C_1(x_1) C_1(x_2) C_1(x_3) \Phi_{111,\text{sub}} \Psi_{\text{sub}}, \tag{77}
\end{aligned}$$

where in the last step we have introduced the subtracted renormalization constants, as well as the subtracted LFWF and lattice factor. If each quark carries a fraction x_q of the longitudinal momentum of the hadron P^+ , for each leg of the LFWF the subtracted renormalization constant is

$$Z_{U_1,\text{sub};\overline{\text{MS}}}\left(\frac{\zeta_q}{\mu^2}\right) = 1 + a_s C_F \frac{1}{\epsilon} \left(\frac{1}{\epsilon} + \frac{3}{2} - \ln\left(\frac{\zeta_q}{\mu^2}\right) - 2 \ln(\text{isign}(L) \text{sign}(x_q)) \right) + \mathcal{O}(a_s^2), \tag{78}$$

with

$$\zeta_q = 2 (x_q P^+)^2 \frac{\nu_q^-}{\nu_q^+}. \tag{79}$$

For each leg of the lattice factor, the renormalization constant is instead

$$Z_{\Psi_1,\text{sub};\overline{\text{MS}}}\left(\frac{\bar{\zeta}_q}{\mu^2}\right) = 1 + a_s C_F \frac{1}{\epsilon} \left(1 - \ln\left(\frac{\bar{\zeta}_q}{\mu^2}\right) \right) + \mathcal{O}(a_s^2), \tag{80}$$

with

$$\bar{\zeta}_q = 2 \frac{(\mu v^-)^2 \nu_q^+}{-v^2 \nu_q^-}. \tag{81}$$

Note that the scales ζ_q and $\bar{\zeta}_q$ are Lorentz invariant, and we have

$$\Phi_{111,\text{sub}}(\{x_q, b_q\}) = \Phi_{111,\text{sub}}(\{x_q, b_q\}, \mu, \{\zeta_q\}) = \frac{\Phi_{111}(\{x_q, b_q\}, \mu, \{\nu_q^+\})}{S_0^{\frac{1}{2}}(\{\nu_q^2\})}, \tag{82}$$

$$\Psi_{\text{sub}}(\{b_q\}) = \Psi_{\text{sub}}(\{b_q\}, \mu, \{\bar{\zeta}_q\}) = \frac{\Psi(\{b_q\}, \mu, \{\nu_q^-\})}{S_0^{\frac{1}{2}}(\{\nu_q^2\})}. \tag{83}$$

To prove that each leg of the factorized QTMD correlator is individually finite, we need the divergent part of the NLO CF (30), which, in the $\overline{\text{MS}}$ renormalization scheme, is

$$\begin{aligned}
\text{pole}[C_{1,\text{NLO}}(x)]_{\overline{\text{MS}}} &= + \text{pole} \left[2a_s C_F \frac{1-\epsilon}{1-2\epsilon} \Gamma(-\epsilon) \Gamma(2\epsilon) \left(\frac{-v^2 \mu^2 e^{-\gamma_E} e^{2\gamma_E}}{(iss_x 2|x|v^- P^+)^2} \right)^\epsilon \right] \\
&= - \frac{a_s C_F}{\epsilon} \left(\frac{1}{\epsilon} + 1 + \ln\left(\frac{-v^2 \mu^2}{(2xv^- P^+)^2}\right) - 2 \ln(\text{isign}(L) \text{sign}(x)) \right). \tag{84}
\end{aligned}$$

We also need the renormalization constant for the semicompact operator (4), i.e. [2],

$$Z_{J;\overline{\text{MS}}} = 1 + \frac{3}{2} a_s C_F \frac{1}{\epsilon} + \mathcal{O}(a_s^2). \tag{85}$$

Combining Eqs. (78), (80), (84), (85), and using

$$\zeta_q \bar{\zeta}_q = \frac{(2\mu v^- x P^+)^2}{-v^2} = \frac{(2x v^- P^+)^2 \mu^4}{-v^2 \mu^2} \quad (86)$$

for every $q = 1, 2, \dots, N$, we prove the complete cancellation of divergences up to next-to-leading order, i.e.,

$$\text{pole}[C_{1,\text{NLO}}(x_q)]_{\overline{\text{MS}}} + \left(Z_{U1,\text{sub};\overline{\text{MS}}} \left(\frac{\zeta_q}{\mu^2} \right) Z_{\Psi1,\text{sub};\overline{\text{MS}}} \left(\frac{\bar{\zeta}_q}{\mu^2} \right) Z_{J;\overline{\text{MS}}}^{-1} \right)_{\text{NLO}} = 0. \quad (87)$$

After subtracting the poles, the remaining finite CF is given by

$$\begin{aligned} C_{1,\text{fin};\overline{\text{MS}}}(x) &= 1 - a_s C_F \left(2 + \frac{5\pi^2}{12} + \ln \left(\frac{-v^2 \mu^2}{(i s s_x 2|x|v^- P^+)^2} \right) + \frac{1}{2} \ln^2 \left(\frac{-v^2 \mu^2}{(i s s_x 2|x|v^- P^+)^2} \right) \right) + \mathcal{O}(a_s^2) \\ &= 1 - a_s C_F \left(2 + \frac{5\pi^2}{12} + \ln \left(\frac{-v^2 \mu^2}{(2x v^- P^+)^2} \right) + \frac{1}{2} \ln^2 \left(\frac{-v^2 \mu^2}{(2x v^- P^+)^2} \right) \right. \\ &\quad \left. - 2 \ln(i s s_x) + \frac{1}{2} (-2 \ln(i s s_x))^2 \right) + \mathcal{O}(a_s^2). \end{aligned} \quad (88)$$

Since

$$2 \ln(i s s_x) = 2 s s_x i \frac{\pi}{2} = s s_x i \pi, \quad (89)$$

we can separate the real part of the CF from the imaginary part, i.e.,

$$\begin{aligned} C_{1,\text{fin};\overline{\text{MS}}}(x) &= 1 + a_s C_F \left(\frac{\pi^2}{12} - 2 - \ln \left(\frac{-v^2 \mu^2}{(2x v^- P^+)^2} \right) - \frac{1}{2} \ln^2 \left(\frac{-v^2 \mu^2}{(2x v^- P^+)^2} \right) \right) \\ &\quad + a_s C_F i \pi \text{sign}(L) \text{sign}(x) + \mathcal{O}(a_s^2). \end{aligned} \quad (90)$$

Therefore, the renormalized QTMD correlator factorizes as

$$\Omega_v(\{x_q, b_q\}, \mu, L) = \Psi_{\text{sub}}(\{b_q\}, \mu, \{\bar{\zeta}_q\}) \mathcal{C}_{111}(\{x_q\}) \Phi_{111,\text{sub}}(\{x_q, b_q\}, \mu, \{\zeta_q\}), \quad (91)$$

where, in the $\overline{\text{MS}}$ renormalization scheme and explicitly up to next-to-leading order, the CF for the LP subtracted baryon LFWF is

$$\begin{aligned} \mathcal{C}_{111;\overline{\text{MS}}}(\{x_q\}) &= \prod_{q=1}^3 C_{1,\text{fin};\overline{\text{MS}}}(x_q) = 1 + a_s C_F \left(\frac{\pi^2}{4} - 6 \right) - a_s C_F \sum_{q=1}^3 \left(\ln \left(\frac{-v^2 \mu^2}{(2x_q v^- P^+)^2} \right) + \frac{1}{2} \ln^2 \left(\frac{-v^2 \mu^2}{(2x_q v^- P^+)^2} \right) \right) \\ &\quad + a_s C_F i \pi \text{sign}(L) \sum_{q=1}^3 \text{sign}(x_q) + \mathcal{O}(a_s^2). \end{aligned} \quad (92)$$

Our results naturally extend those in Ref. [2], with a contribution from every possible pair of quarks. Since in our case there is no contraction between Dirac adjoints, the imaginary parts of the individual CFs do not cancel in the overall coefficient.

V. SCALE EVOLUTION

The subtracted LFWF depends on three mass scales associated to rapidity divergences, i.e., ζ_q with $q = 1, 2, 3$, while the subtracted lattice factor depends on the $\bar{\zeta}_q$, and both quantities also depend on the UV renormalization scale μ . We now study how the LFWF evolves with these scales, showing that the evolution equations with respect to each of them are independent. The solution takes an exponential form, with the rapidity-scale evolutions governed by generalizations of the Collins–Soper kernel.

From Eqs. (76), (77), we have

$$\frac{\Phi_{111,\text{bare}}\Psi_{\text{bare}}}{S} = \left(\prod_{q'=1}^3 Z_{U1,\text{sub}}\left(\frac{\zeta_{q'}}{\mu^2}\right) Z_{\Psi1,\text{sub}}\left(\frac{\bar{\zeta}_{q'}}{\mu^2}\right) \right) \Phi_{111,\text{sub}}(\mu, \{\zeta_q\}) \Psi_{\text{sub}}(\mu, \{\bar{\zeta}_q\}). \quad (93)$$

We take the logarithmic derivative with respect to μ^2 of the logarithm of Eq. (93), at fixed value of the rapidity scales. The left-hand side does not depend on the renormalization scales, and, since only the LFWF depends on $\{\zeta_q\}$ and only the lattice factor depends on $\{\bar{\zeta}_q\}$, we find two independent evolution equations. For the LFWF, we have

$$\mu^2 \frac{\partial}{\partial \mu^2} \Phi_{111,\text{sub}}(\mu, \{\zeta_q\}) = \sum_{q'=1}^3 \gamma_{U1}\left(x_{q'}, \frac{\zeta_{q'}}{\mu^2}\right) \Phi_{111,\text{sub}}(\mu, \{\zeta_q\}), \quad (94)$$

where, from Eq. (78), the anomalous dimensions is

$$\begin{aligned} \gamma_{U1}\left(x_q, \frac{\zeta_q}{\mu^2}\right) &= -\mu^2 \frac{1}{Z_{U1,\text{sub}}} \frac{\partial}{\partial \mu^2} Z_{U1,\text{sub}} = -\mu^2 \frac{\partial}{\partial \mu^2} Z_{U1,\text{sub}} + \mathcal{O}(a_s^2) \\ &\stackrel{\overline{\text{MS}}}{=} a_s C_F \left(\frac{3}{2} - \ln \frac{\zeta_q}{\mu^2} - 2 \ln(i \text{sign}(L) \text{sign}(x_q)) \right) + \mathcal{O}(a_s^2). \end{aligned} \quad (95)$$

Similarly, for the lattice factor we find

$$\mu^2 \frac{\partial}{\partial \mu^2} \Psi_{\text{sub}}(\mu, \{\bar{\zeta}_q\}) = \sum_{q'=1}^3 \gamma_{\Psi1}\left(\frac{\bar{\zeta}_{q'}}{\mu^2}\right) \Psi_{\text{sub}}(\mu, \{\bar{\zeta}_q\}), \quad (96)$$

where, using Eq. (80), the anomalous dimension is

$$\begin{aligned} \gamma_{\Psi1}\left(\frac{\bar{\zeta}_q}{\mu^2}\right) &= -\mu^2 \frac{1}{Z_{\Psi1,\text{sub}}} \frac{\partial}{\partial \mu^2} Z_{\Psi1,\text{sub}} = -\mu^2 \frac{\partial}{\partial \mu^2} Z_{\Psi1,\text{sub}} + \mathcal{O}(a_s^2) \\ &\stackrel{\overline{\text{MS}}}{=} +a_s C_F \left(1 - \ln \frac{\bar{\zeta}_q}{\mu^2} \right) + \mathcal{O}(a_s^2). \end{aligned} \quad (97)$$

From Eq. (86), we have that $\zeta_q, \bar{\zeta}_q$ are not independent when μ is fixed. Therefore, to derive the rapidity-scale evolution of the LFWF, we consider

$$\Phi_{111,\text{bare}} = \left(\prod_{q'=1}^3 R\left(\frac{\delta^+}{\nu_{q'}^+}\right) Z_{U1}\left(\frac{\delta^+}{p_{q'}^+}\right) \right) \Phi_{111}(\mu, \{\nu_q^+\}). \quad (98)$$

From Eq. (79), we have

$$\zeta_q \frac{\partial}{\partial \zeta_q} = -\nu_q^+ \frac{\partial}{\partial \nu_q^+}. \quad (99)$$

Taking the logarithmic derivative with respect to ν^+ of Eq. (98), we have

$$\begin{aligned} &+ \nu_q^+ \frac{\partial \ln\left(R\left(\frac{\delta^+}{\nu_q^+}\right)\right)}{\partial \nu_q^+} \Phi_{111}(\mu, \{\nu_q^+\}) = -\nu_q^+ \frac{\partial}{\partial \nu_q^+} \Phi_{111}(\mu, \{\nu_q^+\}) \\ &= -S_0^{\frac{1}{2}}(\{\nu_q^2\}) \nu_q^+ \frac{\partial}{\partial \nu_q^+} \Phi_{111,\text{sub}}(\mu, \{\zeta_q\}) - \nu_q^+ \frac{\partial S_0^{\frac{1}{2}}(\{\nu_q^2\})}{\partial \nu_q^+} \Phi_{111,\text{sub}}(\mu, \{\zeta_q\}), \end{aligned} \quad (100)$$

where in the last equality we used Eq. (82). Deriving the second equality in Eq. (74) and using Eqs. (67), (68), we also have

$$\nu_q^\pm \frac{\partial S_0^{\frac{1}{2}}(\{\nu_q^2\})}{\partial \nu_q^\pm} = \frac{1}{S_0^{\frac{1}{2}}(\{\nu_q^2\})} \frac{\nu_q^\pm}{2} \frac{\partial S_0(\{\nu_q^2\})}{\partial \nu_q^\pm} = S_0^{\frac{1}{2}}(\{\nu_q^2\}) \frac{\nu_q^\pm}{2} \frac{\partial \ln(S_0(\{\nu_q^2\}))}{\partial \nu_q^\pm} = -S_0^{\frac{1}{2}}(\{\nu_q^2\}) \frac{\nu_q^\pm}{2} \frac{\partial \ln\left(R\left(\frac{\delta^\pm}{\nu_q^\pm}\right)\right)}{\partial \nu_q^\pm}. \quad (101)$$

Combining Eqs. (99)–(101), we find

$$\zeta_q \frac{\partial}{\partial \zeta_q} \Phi_{111,\text{sub}}(\mu, \{\zeta_q\}) = \frac{\nu_q^+}{2} \frac{\partial \ln\left(R\left(\frac{\delta^+}{\nu_q^+}\right)\right)}{\partial \nu_q^+} \Phi_{111,\text{sub}}(\mu, \{\zeta_q\}). \quad (102)$$

Note that, using Eq. (68), we have

$$-\frac{\nu_q^+}{2} \frac{\partial \ln\left(R\left(\frac{\delta^+}{\nu_q^+}\right)\right)}{\partial \nu_q^+} = \frac{1}{4} \sum_{\substack{w=1 \\ w \neq q}}^3 \mathcal{D}\left((b_q - b_w)^2, \mu\right), \quad (103)$$

where

$$\mathcal{D}_{\overline{\text{MS}}}(b^2, \mu) = +2a_s C_F \ln\left(\frac{-b^2}{4}\mu^2\right) + \mathcal{O}(a_s^2) \quad (104)$$

is the standard Collins–Soper kernel.

The integrability conditions follow from the commutativity of the partial derivatives. From Eq. (102) and the fact that the left-hand side of Eq. (103) is independent of the rapidity scales, second order derivatives with respect to these scales vanish, and therefore the corresponding first-order derivatives commute. Moreover, consistency between Eqs. (94) and (102) requires

$$\zeta_q \frac{\partial \gamma_{U1}\left(x_q, \frac{\zeta_q}{\mu^2}\right)}{\partial \zeta_q} = -\mu^2 \frac{\partial}{\partial \mu^2} \left(-\frac{\nu_q^+}{2} \frac{\partial \ln\left(R\left(\frac{\delta^+}{\nu_q^+}\right)\right)}{\partial \nu_q^+} \right), \quad (105)$$

which is indeed satisfied, since, using Eqs. (95), (103), (104), we find

$$\begin{aligned} -\mu^2 \frac{\partial}{\partial \mu^2} \left(-\frac{\nu_q^+}{2} \frac{\partial \ln\left(R\left(\frac{\delta^+}{\nu_q^+}\right)\right)}{\partial \nu_q^+} \right) &= -\frac{1}{4} \sum_{\substack{w=1 \\ w \neq q}}^3 \mu^2 \frac{\partial \mathcal{D}\left((b_q - b_w)^2, \mu\right)}{\partial \mu^2} \\ &= -\frac{1}{4} \sum_{\substack{w=1 \\ w \neq q}}^3 \frac{\Gamma_{\text{cusp}}}{2} = -\frac{1}{4} \Gamma_{\text{cusp}} \overline{\text{MS}} = -a_s C_F + \mathcal{O}(a_s^2) \overline{\text{MS}} \zeta_q \frac{\partial \gamma_{U1}\left(x_q, \frac{\zeta_q}{\mu^2}\right)}{\partial \zeta_q}, \end{aligned} \quad (106)$$

where Γ_{cusp} is the standard cusp anomalous dimension, and in the explicit expression we only kept nonzero terms in the limit $\epsilon \rightarrow 0$.

Finally, combining Eqs. (94), (102), (103), we find

$$d \ln \Phi_{111,\text{sub}}(\mu, \{\zeta_q\}) = \sum_{q=1}^3 \gamma_{U1}\left(x_q, \frac{\zeta_q}{\mu^2}\right) \frac{d\mu^2}{\mu^2} - \frac{1}{4} \sum_{\substack{q,w=1 \\ w \neq q}}^3 \mathcal{D}\left((b_q - b_w)^2, \mu\right) \frac{d\zeta_q}{\zeta_q}, \quad (107)$$

whose solution can be written as

$$\Phi_{111,\text{sub}}(\mu, \{\zeta_q\}) = \Phi_{111,\text{sub}}(\mu_0, \{\zeta_{q,0}\}) P \exp \int \left(\sum_{q=1}^3 \gamma_{U1}\left(x_q, \frac{\zeta_q}{\mu^2}\right) \frac{d\mu^2}{\mu^2} - \frac{1}{4} \sum_{\substack{q,w=1 \\ w \neq q}}^3 \mathcal{D}\left((b_q - b_w)^2, \mu\right) \frac{d\zeta_q}{\zeta_q} \right), \quad (108)$$

where the path-ordered exponential is evaluated between some initial scales $(\mu_0, \{\zeta_{q,0}\})$ and $(\mu, \{\zeta_q\})$.

We are free to choose the path of integration in Eq. (108), e.g., we can evolve each ζ_q independently from all other scales, and in the end evolve μ at fixed values of the rapidity scales. First, we have

$$\exp \int_{\zeta_{q,0}}^{\zeta_q} \frac{d\zeta_q''}{\zeta_q''} \left(-\frac{1}{4} \sum_{\substack{w=1 \\ w \neq q'}}^3 \mathcal{D}\left((b_{q'} - b_w)^2, \mu\right) \right) = \left(\frac{\zeta_q}{\zeta_{q,0}} \right)^{-\frac{1}{4} \sum_{\substack{w=1 \\ w \neq q'}}^3 \mathcal{D}\left((b_{q'} - b_w)^2, \mu\right)}. \quad (109)$$

Therefore, we have

$$\Phi_{111,\text{sub}}(\mu, \{\zeta_q\}) = \left(\prod_{q=1}^3 \left(\frac{\zeta_q}{\zeta_{q,0}} \right)^{-\frac{1}{4} \sum_{\substack{w=1 \\ w \neq q'}}^3 \mathcal{D}\left((b_{q'} - b_w)^2, \mu\right)} \exp \int \frac{d\mu^2}{\mu^2} \gamma_{U1}\left(x_q, \frac{\zeta_q}{\mu^2}\right) \right) \Phi_{111,\text{sub}}(\mu_0, \{\zeta_{q,0}\}). \quad (110)$$

VI. CONCLUSIONS

In this work, we have developed a framework to connect light-front wave functions (LFWFs) of baryons such as the proton to equal-time correlators suitable for Lattice QCD simulations. Building on established factorization approaches for transverse-momentum-dependent (TMD) distributions and meson LFWFs, we have constructed the quasi-transverse-momentum-dependent (QTMD) correlator that can be matched to a light-front amplitude through a TMD operator expansion based on the background field method.

Focusing on the leading three-quark color-singlet LFWF, we have established its factorization theorem from the QTMD correlator up to next-to-leading order. At the bare level, the factorized expression consists of the LFWF and a residual lattice-dependent factor. Both develop additional ultraviolet (UV) and rapidity divergences compared to the original QTMD correlator, the latter being generated by interactions at infinity with lightlike Wilson lines. We have shown how these divergences are canceled one by one by an appropriate soft factor, allowing for a well-defined physical LFWF independently of the residual lattice factor.

The resulting LFWF is multiplicatively renormalizable quark leg by quark leg, and depends on a UV renormalization scale as well as one rapidity scale for each quark. The corresponding scale evolutions are independent, and can be organized within renormalization-group equations. In particular, the rapidity evolutions are governed by generalized Collins–Soper kernels. The evolution exponentiates and reflects the pairwise color correlations characteristic of baryons.

Although explicit calculations were carried out in a specific gauge, the resulting factorization and evolution structure is general, and naturally extends known results for TMD parton distributions and fragmentation functions to the richer color structure of a baryon.

The approach presented in this paper opens up several directions for future work. On the theoretical side, a detailed study of higher Fock components and their mixing under renormalization would help clarify how multi-parton correlations emerge in the proton wave function. It will also be important to investigate the stability of the factorization framework beyond next-to-leading order, and to explore possible simplifications for practical lattice implementations. On the numerical side, the next step is the explicit computation of the proposed correlators in lattice simulations. This requires a careful analysis of systematic effects such as finite-volume corrections, discretization errors, and the treatment of large hadron momenta. A quantitative extraction of proton LFWFs would allow direct comparisons with phenomenological models, and provide new input for the interpretation of experimental observables. More broadly, establishing a reliable method to determine baryon LFWFs from lattice QCD would strengthen the link between first-principle calculations and the parton description of hadron structure. Since many measurable quantities can be understood in terms of LFWFs, access to the wave functions themselves would provide a unified and more detailed picture of the internal dynamics of the proton.

Appendix A: Notations and Conventions

In this appendix, we compile the definitions and conventions used throughout the manuscript, together with some useful relations.

We decompose a generic four-vector $a = (a^+, a^-, \vec{a}_\perp)$ in terms of two light-like vectors \bar{n}, n and a transverse part $a_\perp = (0, 0, \vec{a}_\perp)$, so that

$$\bar{n}^2 = 0 = n^2, \quad \bar{n}n = 1, \quad a_\perp^2 \leq 0, \quad \bar{n}a_\perp = 0 = na_\perp, \quad \bar{n}a = a^-, \quad na = a^+. \quad (\text{A1})$$

The following operators acting on spinor fields form a complete set of orthonormal projectors:

$$\Lambda_+ = \frac{1}{2}\gamma^-\gamma^+ = \frac{1}{\sqrt{2}}\gamma^0\gamma^+, \quad (\text{A2})$$

$$\Lambda_- = \frac{1}{2}\gamma^+\gamma^- = \frac{1}{\sqrt{2}}\gamma^0\gamma^-, \quad (\text{A3})$$

where γ^\pm, γ^0 are Dirac matrices.

The propagator for a Dirac fermion in position space and $D = 4 - 2\epsilon$ dimensions is

$$\overline{\psi_i(a)}\psi_j(b) = \frac{i}{2\pi^{\frac{D}{2}}}\Gamma(2-\epsilon) \frac{\not{a} - \not{b}}{\left(- (a-b)^2 + i0\right)^{2-\epsilon}} \delta_{ij}, \quad (\text{A4})$$

while the gauge-boson propagator is

$$\overline{A_\mu^I(a)}A_\nu^J(b) = \frac{-1}{4\pi^{\frac{D}{2}}}\Gamma(1-\epsilon) \frac{g_{\mu\nu}}{\left(- (a-b)^2 + i0\right)^{1-\epsilon}} \delta^{IJ}, \quad (\text{A5})$$

where i, j, I, J are color indices, and Γ is the Euler Gamma function.

For a $SU(N)$ gauge group with generators $\{t^A\}_{A=1,2,\dots,N^2-1}$ in the fundamental representation, the color algebra satisfies,

$$\sum_{A=1}^{N^2-1} t_{ij}^A t_{kl}^A = \frac{1}{2} \left(\delta_{il} \delta_{jk} - \frac{1}{N} \delta_{ij} \delta_{kl} \right). \quad (\text{A6})$$

We further define the quadratic Casimir multiplicative operator in the fundamental representation as

$$C_F = \frac{N^2 - 1}{2N}. \quad (\text{A7})$$

In dimensional regularization, with $D = 4 - 2\epsilon$ dimensions, we define

$$a_s = \frac{\alpha_s}{(4\pi)^{1-\epsilon}} = \frac{g^2}{(4\pi)^{2-\epsilon}}, \quad (\text{A8})$$

where g is the strong coupling constant. In the $\overline{\text{MS}}$ renormalization scheme, the factor $(4\pi)^\epsilon$ cancels, and we extract a factor of μ^ϵ from the coupling constant, with μ a mass scale, but we keep the same notation for simplicity. We define the anomalous dimension associated with a renormalization constant Z as

$$\gamma = -\mu^2 \frac{\partial \ln Z}{\partial \mu^2} \approx -\mu^2 \frac{\partial Z}{\partial \mu^2}, \quad (\text{A9})$$

where the approximate equality follows from the perturbative expansion

$$Z = 1 + \mathcal{O}(a_s). \quad (\text{A10})$$

-
- [1] A. A. Vladimirov and A. Schäfer, Transverse momentum dependent factorization for lattice observables, *Phys. Rev. D* **101**, 074517 (2020), arXiv:2002.07527 [hep-ph].
- [2] S. Rodini and A. Vladimirov, Factorization for quasi-TMD distributions of sub-leading power, *JHEP* **09**, 117, arXiv:2211.04494 [hep-ph].
- [3] K. Cichy and M. Constantinou, A guide to light-cone PDFs from Lattice QCD: an overview of approaches, techniques and results, *Adv. High Energy Phys.* **2019**, 3036904 (2019), arXiv:1811.07248 [hep-lat].
- [4] X. Ji, Y.-S. Liu, Y. Liu, J.-H. Zhang, and Y. Zhao, Large-momentum effective theory, *Rev. Mod. Phys.* **93**, 035005 (2021), arXiv:2004.03543 [hep-ph].
- [5] M. Constantinou, The x-dependence of hadronic parton distributions: A review on the progress of lattice QCD, *Eur. Phys. J. A* **57**, 77 (2021), arXiv:2010.02445 [hep-lat].
- [6] H.-W. Lin, Mapping parton distributions of hadrons with lattice QCD, *Prog. Part. Nucl. Phys.* **144**, 104177 (2025), arXiv:2506.05025 [hep-lat].
- [7] X. Ji and Y. Liu, Computing light-front wave functions without light-front quantization: A large-momentum effective theory approach, *Phys. Rev. D* **105**, 076014 (2022), arXiv:2106.05310 [hep-ph].
- [8] Z.-F. Deng, W. Wang, and J. Zeng, Transverse-momentum-dependent wave functions and soft functions at one-loop in large momentum effective theory, *JHEP* **09**, 046, arXiv:2207.07280 [hep-th].
- [9] M.-H. Chu *et al.* (Lattice Parton), Transverse-momentum-dependent wave functions of the pion from lattice QCD, *Phys. Rev. D* **109**, L091503 (2024), arXiv:2302.09961 [hep-lat].
- [10] L. F. Abbott, Introduction to the Background Field Method, *Acta Phys. Polon. B* **13**, 33 (1982).
- [11] A. Vladimirov, V. Moos, and I. Scimemi, Transverse momentum dependent operator expansion at next-to-leading power, *JHEP* **01**, 110, arXiv:2109.09771 [hep-ph].
- [12] M. G. Echevarria, I. Scimemi, and A. Vladimirov, Universal transverse momentum dependent soft function at NNLO, *Phys. Rev. D* **93**, 054004 (2016), arXiv:1511.05590 [hep-ph].
- [13] A. Vladimirov, Structure of rapidity divergences in multi-parton scattering soft factors, *JHEP* **04**, 045, arXiv:1707.07606 [hep-ph].